The AAPS Journal (2024) 26:70
https://doi.org/10.1208/s12248-024-00940-8

RESEARCH ARTICLE

3-CMC, 4-CMC, and 4-BMC Human Metabolic Profiling: New Major Pathways to Document Consumption of Methcathinone Analogues?

Diletta Berardinelli[1] · Omayema Taoussi[1] · Gloria Daziani[1] · Francesco Tavoletta[1] · Giovanna Ricci[2] · Livio P. Tronconi[3,4] · Piotr Adamowicz[5] · Francesco P. Busardò[1] · Jeremy Carlier[1]

Received: 25 March 2024 / Accepted: 31 May 2024

Abstract

Synthetic cathinones represent one of the largest and most abused new psychoactive substance classes, and have been involved in numerous intoxications and fatalities worldwide. Methcathinone analogues like 3-methylmethcathinone (3-MMC), 3-chloromethcathinone (3-CMC), and 4-CMC currently constitute most of synthetic cathinone seizures in Europe. Documenting their consumption in clinical/forensic casework is therefore essential to tackle this trend. Targeting metabolite markers is a go-to to document consumption in analytical toxicology, and metabolite profiling is crucial to support investigations. We sought to identify 3-CMC, 4-CMC, and 4-bromomethcathinone (4-BMC) human metabolites. The substances were incubated with human hepatocytes; incubates were screened by liquid chromatography-high-resolution tandem mass spectrometry and data were mined with Compound Discoverer (Themo Scientific). 3-CMC-positive blood, urine, and oral fluid and 4-CMC-positive urine and saliva from clinical/forensic casework were analyzed. Analyses were supported by metabolite predictions with GLORYx freeware. Twelve, ten, and ten metabolites were identified for 3-CMC, 4-CMC, and 4-BMC, respectively, with similar transformations occurring for the three cathinones. Major reactions included ketoreduction and *N*-demethylation. Surprisingly, predominant metabolites were produced by combination of *N*-demethylation and ω-carboxylation (main metabolite in 3-CMC-positive urine), and combination of β-ketoreduction, oxidative deamination, and *O*-glucuronidation (main metabolite in 4-CMC-positive urine). These latter metabolites were detected in negative-ionization mode only and their non-conjugated form was not detected after glucuronide hydrolysis; this metabolic pathway was never reported for any methcathinone analogue susceptible to undergo the same transformations. These results support the need for comprehensive screening strategies in metabolite identification studies, to avoid overlooking significant metabolites and major markers of consumption.

Keywords 3-bromomethcathinone (4-BMC · Brephedrone) · 3-chloromethcathinone (3-CMC) · 4-chloromethcathinone (4-CMC · Clephedrone) · human metabolism · synthetic cathinone

Introduction

Synthetic cathinones (SCs) represent one of the main new psychoactive substance (NPS) classes, along with synthetic cannabinoids and opioids. Generally marketed as legal alternative to illicit drugs, SCs are often sold labeled as "bath salts" and as replacements of popular stimulants, like amphetamines and analogues. SCs such as 3-methylmethcathinone (3-MMC), 3-chloromethylcathinone (3-CMC), and 4-CMC (clephedrone) constitute a large portion of total NPS seizures in the European drug market. Notably, in 2021, SC seizures represented more than 50% of the seized material, 3-CMC and 4-CMC accounting for 34 and 6%, respectively (1, 2). As amphetamine analogues, they

✉ Francesco P. Busardò
f.p.busardo@staff.univpm.it

1 Department of Biomedical Sciences and Public Health, Section of Legal Medicine, Marche Polytechnic University, Ancona, Italy

2 School of Law, Section of Legal Medicine, University of Camerino, Camerino, Italy

3 Department of Public Health, Experimental and Forensic Medicine, Unit of Forensic Medicine, University of Pavia, Pavia, Italy

4 Maria Cecilia Hospital, Cotignola, Italy

5 Jan Sehn Institute of Forensic Research, Cracow, Poland

Published online: 11 June 2024

have stimulant and euphoric properties similar to those of 3,4-methylenedioxymethamphetamine (MDMA) or cocaine. However, they can also cause several adverse effects such as agitation, accelerated heart rate, high blood pressure, unconsciousness, and hallucination (3, 4). These effects are attributed to the SC affinity for dopamine, norepinephrine, and serotonin transporters, increasing the concentration of catecholamines in the central nervous system (1, 5).

Since their appearance in the 2000s, many different SCs emerged onto the illicit drug market with minor modifications at the backbone structure to circumvent legal controls and analytical detection while inducing similar or more potent effects (6). Notably, para- and meta-substituted methcathinones appeared to be highly potent alternatives to the classic cathinones (Fig. 1). In particular, *in vivo* investigations in rats demonstrated that halogenated derivatives exhibit dose- and time-dependent modulation of dopamine brain levels, with 4-CMC being more potent than 4-fluoromethcathinone (4-FMC) and 4-bromomethcathinone (4-BMC, brephedrone) (6, 7). Further studies are necessary to understand the differences in their pharmaco-toxicological profiles (4, 6–8). However, despite the health risks associated with their consumption, SCs have gained great popularity and several intoxications and fatalities related to halogenated SCs have been recently reported (1, 6, 9–15). Particularly, many cases involved 4-CMC consumption along with other NPSs. 3-CMC fatal cases were also reported (11–13, 15, 16).

Due to their extensive metabolic degradation, detection of new emerging SCs challenges analytical toxicologists (5, 17). The detection of metabolites is therefore a go-to to prove consumption in clinical and forensic casework. 4-FMC human metabolism was previously assessed (17). 3- and 4-CMC metabolic transformations have been recently studied, although the investigations were partial (5, 16, 18). To the best of our knowledge, 4-BMC metabolism has not been studied. Our investigation of the metabolism of SCs and search for alternative markers of consumption included the assessment of the human metabolism of 3-CMC, 4-CMC, and 4-BMC using *in silico* metabolite predictions, ten-donor-pooled human hepatocytes incubations, and 3-CMC- and 4-CMC-postive samples from authentic clinical and forensic cases. Incubates and samples were analyzed by liquid chromatography-high-resolution tandem mass spectrometry (LC-HRMS/MS) with positive and negative electrospray ionization, and data were automatically and manually mined for an exhaustive screening of phase I and phase II metabolites.

Experimental

In Silico Metabolite Prediction

Phase I and phase II putative metabolites of 3-CMC, 4-CMC, and 4-BMC were predicted using a machine-learning based tool, GLORYx freeware (19, 20). All the phase I and II first-generation metabolites generated with a prediction score equal or higher than 25% were reprocessed to simulate second-generation metabolism; the score threshold was established based on previous experiments evaluating several metabolite prediction software (3). Second-generation metabolites scores was multiplied to the score of the corresponding first-generation metabolite to calculate a final score (adjusted score).

Chemicals and Reagents

3-CMC, 4-CMC, and 4-BMC reference standards were obtained from Cayman Chemical (Ann Harbor, MI, USA), and diclofenac was purchased from Sigma Aldrich (Milan, Italy). Standard solutions were solubilized in methanol to 1 mg/mL and stored at −20 °C until the analysis.

Carlo Erba (Cornaredo, Italy) provided LC-MS grade water, acetonitrile, and methanol. LC-MS grade formic acid was purchased from Sigma Aldrich.

Williams' medium E, HEPES buffer (2-[4-(2-hydroxyethyl)-1-piperazinyl]ethanesulfonic acid), and *l*-glutamine were supplied by Sigma Aldrich. Supplemented Williams' Medium E (sWME) was prepared dissolving HEPES and *l*-glutamine at 2 and 20 mmol/L, respectively, in Williams' medium E. The solution was prepared extemporaneously. Thawing medium and cryopreserved ten-donor-pooled human hepatocytes were purchased from Lonza (Basel, Switzerland).

Fig. 1 Synthetic cathinone scaffold

Molecule	R_1	R_2
Cathinone	H	H
Methcathinone	CH_3	H
3-MMC	CH_3	3'-CH_3
4-MMC	CH_3	4'-CH_3
3-CMC	CH_3	3'-Cl
4-CMC	CH_3	4'-Cl
4-BMC	CH_3	4'-Br

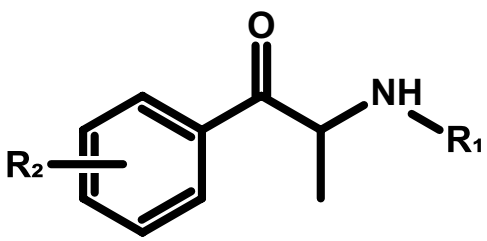

Human Hepatocyte Incubations

As previously described, incubations were conducted following our in-house protocol (21). Briefly, hepatocytes were thawed in thawing medium at 37 °C, then resuspended in sWME. After assessing cell viability with the trypan blue exclusion method, sWME volume was adjusted to 2×10^6 viable cells/mL. The cathinones were diluted to 20 µmol/L in sWME and 250 µL was incubated with 250 µL hepatocytes for 0 or 3 h at 37 °C. Reactions were quenched with an equal volume of ice-cold acetonitrile and centrifugation for 10 min, 15,000 g, at room temperature. The incubates were stored at −80 °C until analysis.

Authentic Samples

Biological samples from three positive cases were analyzed to confirm *in vitro* results. Case #1 was a suicide and was found positive for 3-CMC (70 ng/mL in blood); postmortem blood and urine were collected at the autopsy. Case #2 was an offense of driving under the influence; oral fluid was collected for roadside drug testing positive for both 3- and 4-CMC (non-quantitative). Case #3 was a patient admitted to the hospital and was found positive for 4-CMC (non-quantitative); urine was collected allegedly 3 h after consumption.

Sample Preparation

Hepatocyte Incubations

Incubates were thawed at room temperature, and 100 µL was mixed with 100 µL acetonitrile and centrifuged for 10 min, 15,000 g, at room temperature. The supernatant was dried at 37 °C under a nitrogen stream, reconstituted with 100 µL mobile phases A:B 90:10 (v/v), and centrifuged for 10 min, 15,000 g, at room temperature. The supernatants were transferred into vials with glass inserts and 10 µL was injected onto the chromatographic system.

Authentic Samples

For case #1, 400 µL blood or urine were mixed with 1 mL acetonitrile and centrifuged for 5 min, 15,000 g, at room temperature. The supernatants were evaporated to dryness under nitrogen at 37 °C. The residues were reconstituted with 200 µL mobile phases A:B 90:10 (v/v), and centrifuged for 10 min, 15,000 g, at room temperature. The supernatants were transferred into vials with glass inserts and 10 µL was injected onto the chromatographic system.

For cases #2 (oral fluid) and #3 (urine), samples were thawed at room temperature, and 50 µL was mixed with 150 µL acetonitrile and centrifuged for 10 min, 15,000 g, at room temperature. The supernatants were evaporated to dryness under nitrogen at 37 °C and then followed the same preparative steps as case #1.

Instrumental Conditions

LC-HRMS/MS analysis was performed with a Dionex UltiMate 3000 chromatographic system coupled with a Thermo Scientific (Waltham, MA, USA) Q Exactive mass spectrometer equipped with heated electrospray ionization source. Each sample was injected once in positive- and once in negative-ionization mode.

Liquid Chromatography

Analyte separation was performed through a Kinetex Biphenyl column (150 × 2.1 mm, 2.6 µm) from Phenomenex (Castel Maggiore, Italy) with a mobile phase gradient at 0.4 mL/min composed of 0.1% formic acid in water (A), and 0.1% formic acid in acetonitrile (B). The gradient started with 2% B held for 2 min, increased to 25% B within 12 min, increased to 95% within 2 min, and held for 4 min; initial conditions were restored within 0.1 min and maintained for 3.9 min. The chromatographic run lasted 24 min. The column oven was set at 37 ± 1 °C and the autosampler temperature was 10 ± 1 °C.

High-Resolution Tandem Mass Spectrometry

Source settings were: spray voltage, ±3.5 kV; sheath gas flow rate, 50 arbitrary units (a.u.); auxiliary gas flow rate, 5 a.u.; auxiliary gas temperature, 300 °C; capillary temperature, 300 °C; S-lens radio frequency level, 50 a.u.

The mass spectrometer acquired from 1 to 20 min of the chromatographic run in full-scan HRMS (FullMS)/data dependent MS/MS ($ddMS^2$) mode. FullMS settings were: range, *m/z* 100–500; resolution at full width at half maximum at *m/z* 200, 70,000; automatic gain control (AGC) target, 10^6; and maximum injection time (IT), 200 ms. $ddMS^2$ settings were: AGC target, 2×10^5; maximum IT, 64 ms; isolation window, *m/z* 1.2; resolution, 17,500; and stepped normalized collision energy (NCE), 20, 80, and 100 a.u. A maximum number of five $ddMS^2$ scans were triggered for each FullMS scan (minimum intensity, 10^4; dynamic exclusion, 2.0 s) depending on an inclusion list of putative metabolites based on *in silico* predictions and postulation (Supplementary Table S1) (5, 16, 18). Due to 4-BMC isotopic distribution, the 3-h incubate with hepatocytes was reinjected with two different inclusion lists using ^{79}Br or ^{81}Br isotope to increase the chances to obtain non-interfered HRMS/MS spectra. Ions that were not included in the inclusion list also triggered $ddMS^2$ scans, although they were not priority ("pick others if idle" option). In addition, an exclusion list was compiled based on background noise, as

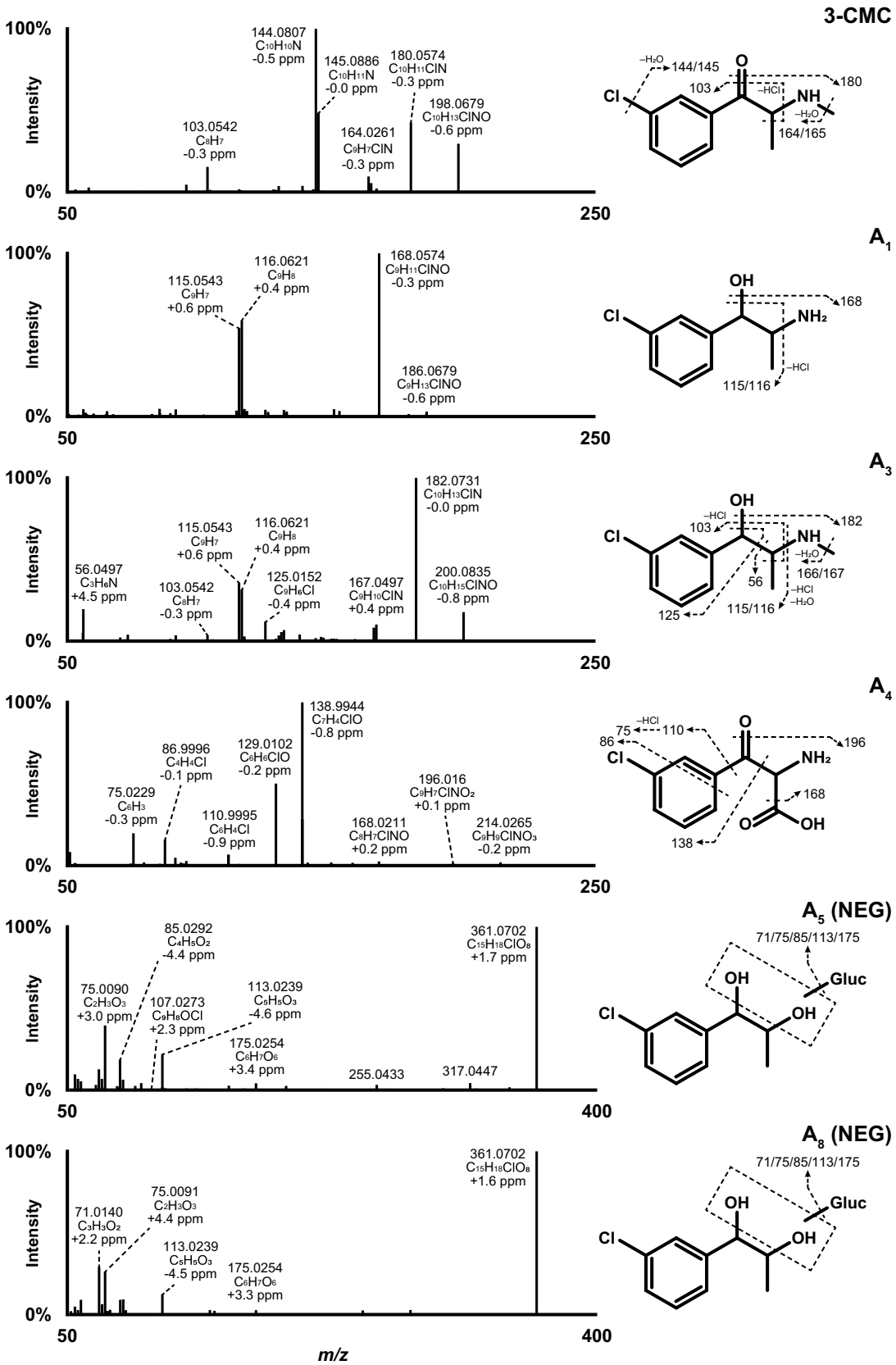
3-CMC
100%
Intensity
0%
50
250
144.0807
C10H10N
-0.5 ppm
145.0886
C10H11N
-0.0 ppm
180.0574
C10H11ClN
-0.3 ppm
198.0679
C10H13ClNO
-0.6 ppm
103.0542
C8H7
-0.3 ppm
164.0261
C9H7ClN
-0.3 ppm
–H2O
144/145
O
180
103
–HCl
NH
–H2O
164/165
Cl
A1
116.0621
C9H8
+0.4 ppm
168.0574
C9H11ClNO
-0.3 ppm
115.0543
C9H7
+0.6 ppm
186.0679
C9H13ClNO
-0.6 ppm
OH
168
NH2
–HCl
115/116
A3
182.0731
C10H13ClN
-0.0 ppm
115.0543
C9H7
+0.6 ppm
116.0621
C9H8
+0.4 ppm
56.0497
C3H6N
+4.5 ppm
103.0542
C8H7
-0.3 ppm
125.0152
C9H6Cl
-0.4 ppm
167.0497
C9H10ClN
+0.4 ppm
200.0835
C10H15ClNO
-0.8 ppm
–HCl
103
182
NH
–H2O
166/167
56
–HCl
–H2O
125
115/116
A4
138.9944
C7H4ClO
-0.8 ppm
86.9996
C4H4Cl
-0.1 ppm
129.0102
C6H6ClO
-0.2 ppm
75.0229
C6H3
-0.3 ppm
110.9995
C6H4Cl
-0.9 ppm
196.016
C9H7ClNO2
+0.1 ppm
168.0211
C8H7ClNO
+0.2 ppm
214.0265
C9H9ClNO3
-0.2 ppm
–HCl
75
110
O
86
196
NH2
168
O
OH
138
A5 (NEG)
400
85.0292
C4H5O2
-4.4 ppm
361.0702
C15H18ClO8
+1.7 ppm
75.0090
C2H3O3
+3.0 ppm
107.0273
C9H8OCl
+2.3 ppm
113.0239
C5H5O3
-4.6 ppm
175.0254
C6H7O6
+3.4 ppm
255.0433
317.0447
71/75/85/113/175
Gluc
OH
OH
A8 (NEG)
361.0702
C15H18ClO8
+1.6 ppm
71.0140
C3H3O2
+2.2 ppm
75.0091
C2H3O3
+4.4 ppm
113.0239
C5H5O3
-4.5 ppm
175.0254
C6H7O6
+3.3 ppm
m/z

◂**Fig. 2** HRMS/MS spectra of 3-CMC and major metabolites identified in human hepatocyte incubates and authentic samples and suggested fragmentation pattern. Unless stated otherwise, spectra were produced after positive electrospray ionization. Gluc, glucuronide; NEG, negative-ionization mode

evaluated during the injection of blank control samples (A:B 90:10, v/v). The Orbitrap was calibrated prior to analysis and a lock mass list with previously identified background ions was compiled in positive-ionization mode and used throughout the analysis for better accuracy (22).

Data Mining

LC-HRMS/MS data mining was performed with Compound Discoverer™ (Thermo Scientific, v. 3.2.0.421), applying a mixed targeted/untargeted workflow as previously described, with minor modifications (3, 23). Briefly, after spectrum selection and retention time alignment between raw data files, the ions were compared to a list of theoretical metabolites generated using combinations of selected transformations. The potential metabolites were then compared to mzCloud, ChemSpider and HighResNPS libraries. Besides, the HRMS/MS spectra and theoretical elemental composition of all ions with an intensity higher than 10^5 were compared to the same databases. For each sample, signals with an intensity lower than 1% of the most intense metabolite identified were not considered.

Results

In Silico Metabolite Prediction

Predictions of 3-CMC, 4-CMC, and 4-BMC phase I and phase II metabolites in humans are displayed in Supplementary Table S2. A total of 9 first-generation (pA_1-pA_9) and 64 second-generation ($pA_{X\text{-}1}$ to $pA_{X\text{-}13}$, pA_X representing the corresponding first-generation metabolite) metabolites were predicted for 3-CMC; 20 metabolites were duplicates. A total of 9 first-generation (pB_1-pB_9) and 48 second-generation ($pB_{X\text{-}1}$-$pB_{X\text{-}13}$) metabolites were predicted for 4-CMC, 12 being duplicates. A total of 10 first-generation (pC_1-pC_{10}) and 54 second-generation ($pC_{X\text{-}1}$ to $pC_{X\text{-}13}$) metabolites were predicted for 4-BMC, 13 being duplicates. The principal phase I transformations shared by all three analogues were *N*-acetylation, hydroxylation (phenyl ring or alkyl chain), β-ketoreduction, *N*-demethylation, and oxidative deamination.

To favor the acquisition of their product-ion spectra over other compounds during the LC-HRMS/MS analysis, all predicted metabolites were compiled in inclusion lists (Supplementary Table S1). All predicted metabolic reactions and combinations were included in the lists of possible transformations for data mining with Compound Discoverer™.

In Vitro Metabolite Identification

The three analogues were only detected in positive-ionization mode: 3-CMC and 4-CMC eluted at 8.72 and 9.14 min, respectively, with a base peak at *m/z* 198.0678, while 4-BMC was detected at 10.02 min ($[M+H]^+$, *m/z* 242.0173). As expected from structural analogues, 3-CMC, 4-CMC, and 4-BMC displayed similar fragmentation pattern (Figs. 2, 3 and 4), the only significant difference being the relative intensity of the fragment produced by water loss, which was high in 3- and 4-CMC (*m/z* 180.0574), consistent with the literature (5, 18), and low in 4-BMC (*m/z* 224.0067). Subsequent hydrochloric or hydrobromic acid loss produced major fragments at *m/z* 144.0808/145.0886 in all three compounds. Minor fragment at *m/z* 103.0542 corresponded to the phenylethyl moiety.

3- and 4-CMC LC-HRMS area were 70% and 15% lower from 0 to 3 h of incubation, respectively. Nine 3-CMC metabolites (A_1-A_9, by ascending retention time) and nine 4-CMC metabolites (B_1-B_9) were identified. 4-BMC LC-HRMS signal was 40% less intense from 0 h to 3 h of incubation, and ten metabolites (C_1-C_{10}) were identified. Considering that the three molecules were incubated simultaneously and analyzed under the same conditions, the discrepancy observed in the metabolic degradation rates might be explained by a different interaction with metabolic enzymes, cofactors, and transporters based on the halogen nature and position. However, no major differences were observed in the metabolites produced after incubation. β-Ketoreduction and *N*-demethylation were prominent reactions for all three molecules, and metabolites with ω-hydroxylation, ω-carboxylation, *O*-glucuronidation, and/or *N*-acetylation were also detected; metabolites with oxidative deamination were only detected in combination with β-ketoreduction and *O*-glucuronidation. Although the reactions were the same between the three cathinones, beside *N*-acetylation being only identified with 3-CMC, the relative intensity of the metabolites with the same transformation showed better resemblance between 4-CMC and 4-BMC than between 3- and 4-CMC.

In vitro results are reported in Tables II, I, and III. Extracted-ion chromatograms of 3-CMC, 4-CMC, 4-BMC, and their metabolites after positive and negative ionization after incubation are displayed in Fig. 5. Structure elucidation of major metabolites is described below.

β-Ketoreduction

Reduction of the carbonyl group (+2H) generated the most intense metabolites for 3-CMC (A_3), 4-CMC (B_4), and

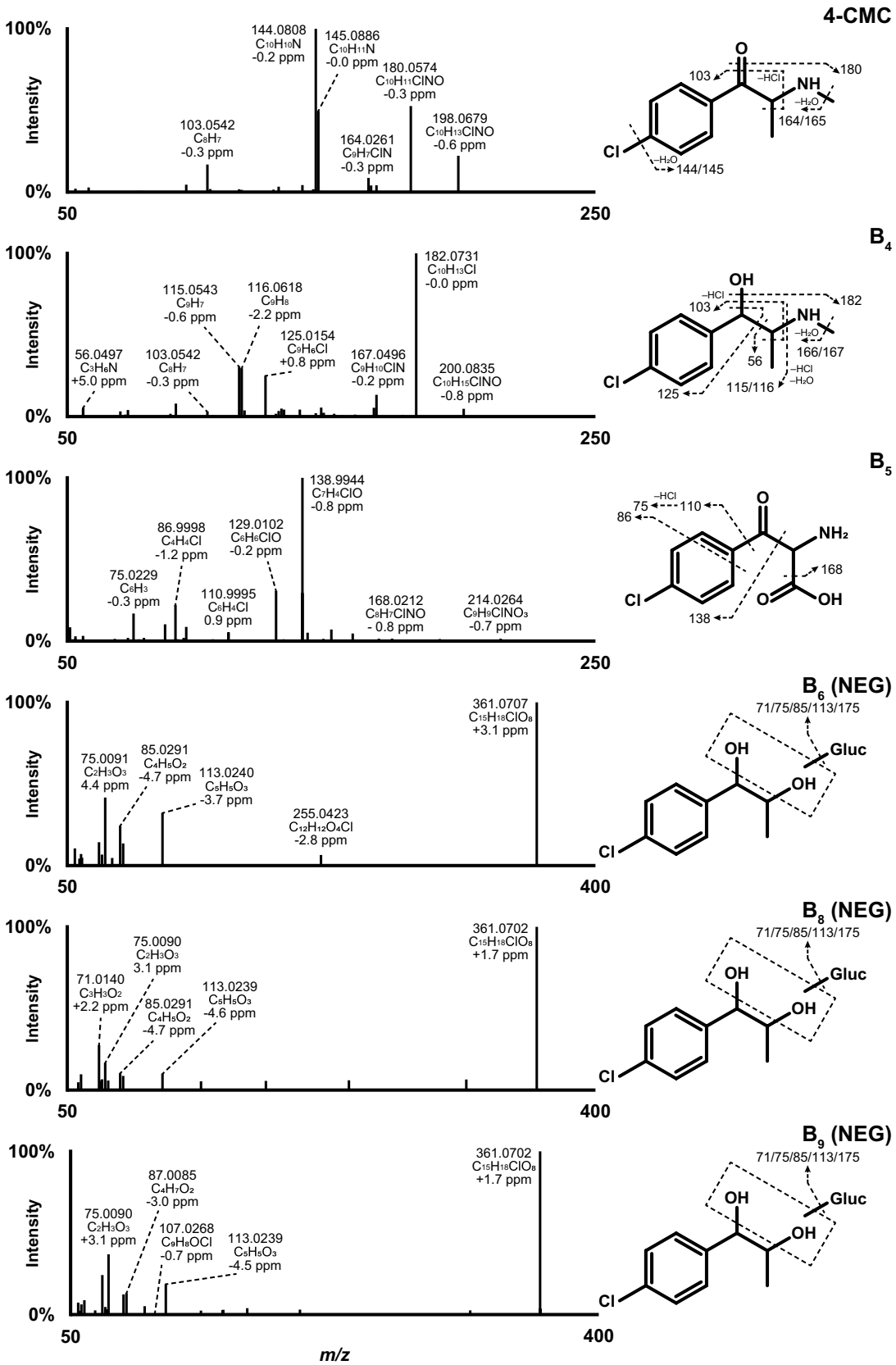
4-CMC
100%
Intensity
0%
50
250
144.0808
C10H10N
-0.2 ppm
145.0886
C10H11N
-0.0 ppm
180.0574
C10H11ClNO
-0.3 ppm
103.0542
C8H7
-0.3 ppm
164.0261
C9H7ClN
-0.3 ppm
198.0679
C10H13ClNO
-0.6 ppm
O
103
–HCl
180
NH
–H2O
164/165
Cl
–H2O
144/145
B4
182.0731
C10H13Cl
-0.0 ppm
115.0543
C9H7
-0.6 ppm
116.0618
C9H8
-2.2 ppm
125.0154
C9H6Cl
+0.8 ppm
56.0497
C3H6N
+5.0 ppm
103.0542
C8H7
-0.3 ppm
167.0496
C9H10ClN
-0.2 ppm
200.0835
C10H15ClNO
-0.8 ppm
OH
–HCl
103
182
NH
–H2O
166/167
56
Cl
125
115/116
–HCl
–H2O
B5
138.9944
C7H4ClO
-0.8 ppm
86.9998
C4H4Cl
-1.2 ppm
129.0102
C6H6ClO
-0.2 ppm
75.0229
C6H3
-0.3 ppm
110.9995
C6H4Cl
0.9 ppm
168.0212
C8H7ClNO
- 0.8 ppm
214.0264
C9H9ClNO3
-0.7 ppm
–HCl
75
110
O
86
NH2
168
Cl
O
OH
138
B6 (NEG)
361.0707
C15H18ClO8
+3.1 ppm
75.0091
C2H3O3
4.4 ppm
85.0291
C4H5O2
-4.7 ppm
113.0240
C5H5O3
-3.7 ppm
255.0423
C12H12O4Cl
-2.8 ppm
400
71/75/85/113/175
OH
Gluc
OH
Cl
B8 (NEG)
361.0702
C15H18ClO8
+1.7 ppm
75.0090
C2H3O3
3.1 ppm
71.0140
C3H3O2
+2.2 ppm
85.0291
C4H5O2
-4.7 ppm
113.0239
C5H5O3
-4.6 ppm
71/75/85/113/175
OH
Gluc
OH
Cl
B9 (NEG)
361.0702
C15H18ClO8
+1.7 ppm
87.0085
C4H7O2
-3.0 ppm
75.0090
C2H3O3
+3.1 ppm
107.0268
C9H8OCl
-0.7 ppm
113.0239
C5H5O3
-4.5 ppm
71/75/85/113/175
OH
Gluc
OH
Cl
m/z

◂**Fig. 3** HRMS/MS spectra of 4-CMC and major metabolites identified in human hepatocyte incubates and authentic samples and suggested fragmentation pattern. Unless stated otherwise, spectra were produced after positive electrospray ionization. Gluc, glucuronide; NEG, negative-ionization mode

4-BMC (C_4) after positive ionization. The transformation was suggested by a + 2.0156 Da ±5 ppm mass shift from the corresponding parent and a substantial in-source water loss, typical of synthetic cathinones with a β-ketoreduction in similar instrumental and analytical conditions (3,24); for B_4, the signal of the in-source fragment was even 20% higher than that of the precursor ion. The water loss was also the most intense fragment in A_3, B_4, and C_4 HRMS/MS spectra, which also contained minor fragments at *m/z* 125.0153 ± 5 ppm (A_3 and B_4) or 168.9646 (C_4) and 115.0542/116.0621 ± 5 ppm, indicating loss of water and methylamine, and further hydrochloric or hydrobromic acid, respectively. Under the present chromatographic conditions, B_4 and C_4 LC-HRMS peaks, from 4-CMC and 4-BMC metabolism, respectively, presented a shoulder, suggesting the coelution of diastereoisomers due to the formation of a chiral center; A_3 from 3-CMC did not present a shoulder.

N-*Demethylation*

Another major transformation was the dealkylation of the *N*-methyl group (-CH_2), which was suggested by a − 14.0157 Da ±5 ppm mass shift from the corresponding parent (A_2, B_3, and C_3 from 3-CMC, 4-CMC, and 4-BMC, respectively). The three metabolites had a fragmentation pattern similar to that of their respective parent in positive-ionization mode with major water loss in 3- and 4-CMC spectra at *m/z* 166.0418 and further hydrochloric or hydrobromic loss at *m/z* 130.0651/131.0730, and fragment at *m/z* 103.0542 corresponding to the phenylethyl moiety for all three compounds.

β-Ketoreduction and N-*Demethylation*

Combination of the two major reactions β-ketoreduction (+2H) and *N*-demethylation (-CH_2) produced another metabolite in 3-CMC (A_1), and two other diastereoisomer metabolites in 4-CMC (B_1 and B_2), and 4-BMC (C_1 and C_2) incubates. The metabolites' structure was elucidated through their −12.0000 Da ±5 ppm mass shift from the corresponding parent, their substantial in-source water loss, and their HRMS/MS spectra displaying previously described fragments at *m/z* 115.0542/116.0621 ± 5 ppm and 168.0575 ± 5 ppm (A_1, B_1, and B_2) or 212.0069 (C_1 and C_2) due to water loss. Under the chromatographic conditions of the analysis, B_1/B_2 and C_1/C_2 diastereoisomers, due to 4-CMC and 4-BMC ketoreduction, respectively, were completely resolved; A_1 from 3-CMC only presented one peak.

N-*Demethylation and ω-Carboxylation*

Although ω-carboxylation (-2H + 2O) alone was not detected with a signal higher than the established threshold, it was found in combination with *N*-demethylation (-CH_2) in 3-CMC (A_4), 4-CMC (B_5), and 4-BMC (C_6) incubates in both positive- and negative-ionization modes. Elemental composition change was indicated by a + 15.9586 Da ±5 ppm mass shift from the respective parent. In negative mode, C_6 fragmentation generated the bromide ion at *m/z* 78.9192; the corresponding fragment was not detected in A_4 and B_5 spectra, the chloride ion having a mass lower than 50 Da. Other intense fragments were found at *m/z* 168.0222 ± 5 ppm (A_4 and B_5) or 211.9722 (C_6) due to formic acid loss, and 111.0007 ± 5 ppm (A_4 and B_5) or 154.9507 (C_6) formed by the chlorophenyl or bromophenyl ions, respectively. In positive-ionization mode, characteristic fragments were produced by α-cleavage on either side of the carbonyl group at *m/z* 110.9995 and 138.9944 for A_4 and B_5, and 154.9492 and 182.9431 for C_6, indicating that the transformation occurred at the methyl. Fragments at *m/z* 129.0102 for A_4 and B_5 and 172.9597 for C_6 were produced by the chloro/bromobenzyl ring after rearrangement to include an oxygen atom, likely from the carboxylic acid group. A_4, B_5, and C_6 ranked first, second, and second most intense metabolites in 3-CMC, 4-CMC, and 4-BMC, respectively, due to their high intensity in negative-ionization mode entailed by the presence of a carboxyl group.

β-Ketoreduction, Oxidative Deamination, and O-*Glucuronidation*

Three metabolites with the same mass and fragmentation pattern were only detected in negative-ionization mode, although with a relatively intense signal, in 3-CMC (A_5, A_6, and A_8), 4-CMC (B_6, B_8, and B_9), and 4-BMC (C_7, C_9, and C_{10}) incubates. These metabolites were produced by oxidative deamination (-NH_2 + OH), *O*-glucuronidation (+$C_6H_8O_6$), and β-ketoreduction (+2H), as suggested by their +163.0016 Da ±5 ppm mass shift from their respective parent; they are the only phase II metabolites detected *in vitro*. The lack of signal in positive-ionization mode, despite their intensity after negative ionization, may be explained be the substitution of the amine group, which is much more prone to carry a positive charge during electrospray ionization. The spectra of the metabolites contained the glucuronide loss at *m/z* 167.0269 ± 5 ppm for 3- and 4-CMC metabolites or 210.9767 ± 5 ppm for 4-BMC and typical ions from the glucuronide fragmentation at *m/z* 71.0139 ± 5 ppm, 75.0087 ± 5 ppm, 85.0295 ± 5 ppm, and 113.0244 ± 5 ppm

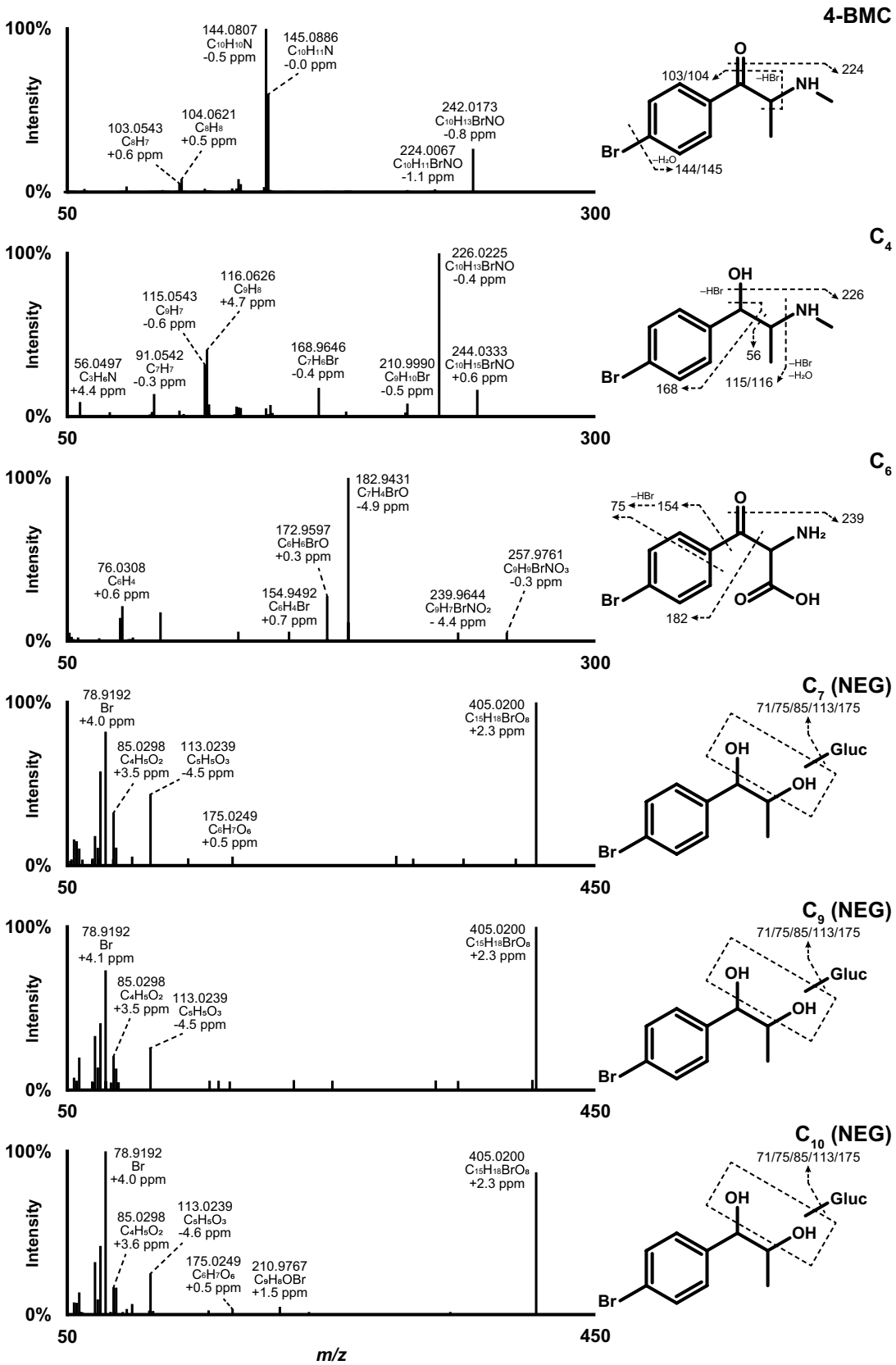

Fig. 4 HRMS/MS spectra of 4-BMC and major metabolites identified in human hepatocyte incubates and suggested fragmentation pattern. Unless stated otherwise, spectra were produced after positive electrospray ionization. Gluc, glucuronide; NEG, negative-ionization mode

Table I Metabolic Transformation, Elemental Composition, Retention time (RT), Accurate Mass of Protonated ($[M+H]^+$) and Deprotonated ($[M-H]^-$) Ion, Deviation from Exact Mass, and Liquid Chromatography-High-Resolution Mass Spectrometry Peak Area of 3-CMC and Metabolites after 3-h Incubation with Human Hepatocytes and in Authentic Samples. Mass Tolerance, 5 ppm

ID	Biotransformation	Elemental composition	RT (min)	*m/z* (Δppm) $[M+H]^+$ $[M-H]^-$	Peak area in incubates $[M+H]^+$ $[M-H]^-$	Blood (case #1)	Urine (case #1)	Oral Fluid (case #2)
A_1	β-Ketoreduction + *N*-Demethylation	$C_9H_{12}ONCl$	7.35	186.0679 (−0.6) ND	6.8×10^6 ND	2.0×10^6 ND	1.2×10^8 ND	2.9×10^8 ND
A_2	*N*-Demethylation	$C_9H_{10}ClNO$	7.96	184.0522 (−0.9) ND	3.9×10^7 ND	ND ND	2.5×10^8 ND	7.4×10^7 ND
A_A	β-Ketoreduction + *O*-glucuronidation	$C_{16}H_{22}ClNO_7$	8.09	376.1158 (+0.1) 374.1018 (+1.6)	ND ND	5.4×10^5 2.6×10^5	6.2×10^7 2.1×10^7	ND ND
A_3	β-Ketoreduction	$C_{10}H_{14}ClNO$	8.59	200.0835 (−0.8) ND	2.4×10^8 ND	2.1×10^8 ND	2.5×10^9 ND	3.3×10^9 ND
A_B	β-Ketoreduction + *O*-glucuronidation	$C_{16}H_{22}ClNO_7$	9.01	376.1158 (+0.1) 374.1018 (+1.6)	ND ND	1.4×10^6 6.6 X 10^5	1.5×10^8 5.9×10^7	ND ND
3-CMC		$C_{10}H_{12}ClNO$	8.74	198.0679 (−0.6) ND	1.8×10^9 ND	ND ND	1.9×10^7 ND	2.5×10^9 ND
A_4	*N*-Demethylation + ω-Carboxylation	$C_9H_8ClNO_3$	10.97	214.0264 (−0.7) 212.0126 (+2.9)	4.8×10^7 2.8×10^8	9.2×10^5 1.1×10^7	1.2×10^8 1.2×10^9	ND 2.8×10^6
A_5	β-Ketoreduction + Oxidative deamination + *O*-Glucuronidation	$C_{15}H_{19}ClO_8$	11.01	ND 361.0703 (+2.0)	ND 3.2×10^7	ND 9.7×10^6	ND 1.9×10^9	ND 3.5×10^5
A_6	β-Ketoreduction + Oxidative deamination + *O*-Glucuronidation	$C_{15}H_{19}ClO_8$	11.42	ND 361.0703 (+2.0)	ND 3.2×10^6	ND 5.6×10^6	ND 4.6×10^8	ND ND
A_7	ω-Hydroxylation	$C_{10}H_{12}ClNO_2$	11.87	214.0628 (−0.6) ND	1.3×10^7 ND	ND ND	ND ND	2.2×10^5 ND
A_8	β-Ketoreduction + Oxidative deamination + *O*-Glucuronidation	$C_{15}H_{19}ClO_8$	11.90	ND 361.0703 (+2.0)	ND 9.2×10^6	ND 5.8×10^7	ND 4.1×10^9	ND 3.3×10^6
A_C	β-Ketoreduction + Oxidative deamination + *O*-Glucuronidation	$C_{15}H_{19}ClO_8$	12.08	ND 361.0703 (+2.0)	ND 1.7×10^{6a}	ND 2.0×10^6	ND 1.7×10^8	ND ND
A_9	β-Ketoreduction + *N*-Acetylation	$C_{12}H_{16}ClNO_2$	15.26	242.0940 (−1.0) ND	2.0×10^7 ND	ND ND	ND ND	ND ND

ND not detected

[a]*retrospectively detected in incubates after identification in real samples*

under similar instrumental and analytical conditions (25,26), C_7, C_9, and C_{10} spectra also contained the bromide ion at *m/z* 78.9189 ± 5 ppm.

A fourth peak with the same *m/z* and fragmentation pattern was manually found with an intensity below the intensity threshold at 12.08, 11.87, and 12.67 min for 3-CMC, 4-CMC, and 4-BMC, respectively (one of these peaks was detected with an intensity above the threshold in the blood and urine of the 3-CMC-positive case #1 and named A_C – see below). Considering that β-ketoreduction may generate two diastereoisomers and, either for 3-CMC, 4-CMC, and 4-BMC, the four metabolites had similar HRMS/MS

Table II Metabolic Transformation, Elemental Composition, Retention Time (RT), Accurate Mass of Protonated ($[M+H]^+$) and Deprotonated ($[M-H]^-$) Ion, Deviation from Exact Mass, and Liquid Chromatography-High-Resolution Mass Spectrometry Peak Area of 4-CMC and Metabolites after 3-h Incubation with Human Hepatocytes and in Authentic Samples. Mass Tolerance, 5 ppm

ID	Biotransformation	Elemental composition	RT, min	*m/z* (Δppm) $[M+H]^+$ $[M-H]^-$	Peak area in incubates $[M+H]^+$ $[M-H]^-$	Oral Fluid (case #2)	Urine (case #3)
B_1	β-Ketoreduction + *N*-Demethylation	$C_9H_{12}ONCl$	7.67	186.0678 (−1.2) ND	5.9×10^6 ND	5.1×10^7 ND	2.5×10^6 ND
B_2	β-Ketoreduction + *N*-Demethylation	$C_9H_{12}ONCl$	7.87	186.0679 (−0.6) ND	2.5×10^6 ND	2.3×10^7 ND	1.1×10^6 ND
B_3	*N*-Demethylation	$C_9H_{10}ClNO$	8.40	184.0523 (−0.4) ND	3.3×10^7 ND	8.0×10^5 ND	7.1×10^6 ND
B_4	β-Ketoreduction	$C_{10}H_{14}ClNO$	8.98	200.0835 (−0.8) ND	3.0×10^8 ND	7.7×10^8 ND	7.8×10^7 ND
4-CMC		$C_{10}H_{12}ClNO$	9.14	198.0679 (−0.6) ND	2.2×10^9 ND	2.5×10^7 ND	4.9×10^8 ND
B_5	*N*-Demethylation + ω-Carboxylation	$C_9H_8ClNO_3$	11.16	214.0264 (−0.7) 212.0126 (+2.9)	1.1×10^7 7.3×10^7	ND ND	1.9×10^7 2.1×10^8
B_6	β-Ketoreduction + Oxidative deamination + *O*-Glucuronidation	$C_{15}H_{19}ClO_8$	11.48	ND 361.0703 (+2.0)	ND 6.2×10^6	ND ND	ND 4.1×10^7
B_7	ω-Hydroxylation	$C_{10}H_{13}ClNO_2$	11.93	214.0629 (−0.2) ND	3.8×10^7 ND	ND ND	ND ND
B_8	β-Ketoreduction + Oxidative deamination + *O*-Glucuronidation	$C_{15}H_{19}ClO_8$	12.21	ND 361.0703 (+2.0)	ND 3.9×10^6	ND ND	ND 5.7×10^7
B_9	β-Ketoreduction + Oxidative deamination + *O*-Glucuronidation	$C_{15}H_{19}ClO_8$	12.53	ND 361.0702 (+1.7)	ND 1.0×10^7	ND ND	ND 5.5×10^7
B_A	Hydroxylation + *O*-Glucuronidation	$C_{16}H_{20}ClNO_8$	13.75	390.0945 (−1.2) 388.0814 (+2.4)	2.9 x 10^{5a} 3.6 x 10^{5a}	ND ND	7.0×10^6 5.7×10^6

ND not detected

[a] *retrospectively detected in incubates after identification in real samples*

spectra, it may be hypothesized that two sets of diastereoisomers (R/S) were produced with *O*-glucuronidation at either one or the other hydroxyl group formed by β-ketoreduction, producing two diastereoisomers (R/S) depending on the configuration of the newly formed asymmetric carbon, and oxidative deamination. The exact position of the glucuronides might be determined with further studies with nuclear magnetic resonance or comparison to analytical standards.

3- and 4-CMC *in Vivo* Metabolite Identification

In vivo results are compiled in Tables I and II. Extracted-ion chromatograms of 3-CMC, 4-CMC, and their metabolites after positive and negative ionization in authentic samples are displayed in Fig. 6.

Case #1: 3-CMC-Positive Blood and Urine

Except for A_2, A_7, and A_9, all 3-CMC metabolites identified in human hepatocyte incubations were also detected in the autoptic blood from case #1; 3-CMC itself was not detected. Except for A_7 and A_9, all metabolites identified *in vitro* were also detected in the urine. Two additional diastereoisomer metabolites (A_A and A_B by ascending retention time) produced by β-ketoreduction (+2H) and glucuronidation ($+C_6H_8O_6$) were identified both in blood and urine, as suggested by their +178.0478 Da mass shift from 3-CMC and their fragmentation spectra that are similar to that of the corresponding non-conjugated metabolite A_3. Another additional metabolite (A_C) produced by β-ketoreduction, oxidative deamination, and *O*-glucuronidation was also identified in blood and urine, as suggested by the +163.0016 Da ±5 ppm mass shift from the parent and the fragmentation similar to that of A_4, A_5, and A_8, which underwent the same transformations; A_C was retrospectively identified in human hepatocyte incubates. A_3 (β-ketoreduction) was the metabolite with the most intense signal in positive-ionization mode in blood, and A_4 (*N*-demethylation and ω-carboxylation) and A_8 (β-ketoreduction, oxidative deamination, and *O*-glucuronidation) were intense only in negative-ionization mode.

Table III Metabolic Transformation, Elemental Composition, Retention Time (RT), Accurate Mass Of Protonated ($[M+H]^+$) and Deprotonated ($[M\text{-}H]^-$) Ion, Deviation from Exact Mass, and Liquid Chromatography-High-Resolution Mass Spectrometry Peak Area of 4-BMC and Metabolites after 3-h Incubation with Human Hepatocytes. Mass Tolerance, 5 ppm

ID	Biotransformation	Elemental composition	RT, min	*m/z* (Δppm) $[M+H]^+$ $[M\text{-}H]^-$	Peak area $[M+H]^+$ $[M\text{-}H]^-$
C_1	β-Ketoreduction + *N*-Demethylation	$C_9H_{12}BrNO$	8.65	230.0174 (−0.4) ND	1.4×10^7 ND
C_2	β-Ketoreduction + *N*-Demethylation	$C_9H_{12}BrNO$	8.79	230.0174 (−0.4) ND	7.4×10^6 ND
C_3	*N*-Demethylation	$C_9H_{10}BrNO$	9.32	228.0018 (−0.2) ND	6.2×10^7 ND
C_4	β-Ketoreduction	$C_{10}H_{14}BrNO$	9.84	244.0330 (−0.6) ND	4.8×10^8 ND
4-BMC		$C_{10}H_{12}BrNO$	10.02	242.0174 (−0.4) ND	2.6×10^9 ND
C_5	β-Ketoreduction + ω-Hydroxylation	$C_{10}H_{14}BrNO_2$	11.46	260.0280 (−0.3) ND	8.7×10^6 ND
C_6	*N*-Demethylation + ω-Carboxylation	$C_9H_8BrNO_3$	12.21	257.9759 (−0.5) 255.9620 (+2.0)	2.6×10^7 1.3×10^8
C_7	β-Ketoreduction + Oxidative deamination + *O*-Glucuronidation	$C_{15}H_{18}BrO_8$	12.24	ND 405.0196 (+1.3)	ND 1.4×10^7
C_8	ω-Hydroxylation	$C_{10}H_{12}BrNO_2$	12.92	258.0123 (−0.5) ND	5.0×10^7 ND
C_9	β-Ketoreduction + Oxidative deamination + *O*-Glucuronidation	$C_{15}H_{18}BrO_8$	13.01	ND 405.0195 (+1.1)	ND 9.0×10^6
C_{10}	β-Ketoreduction + Oxidative deamination + *O*-Glucuronidation	$C_{15}H_{18}BrO_8$	13.31	ND 405.0196 (+1.3)	ND 2.3×10^7

ND not detected

Similarly, A_3 was detected with a high intensity in positive-ionization mode in urine, but A_4, A_5 (β-ketoreduction, oxidative deamination, and *O*-glucuronidation), and A_8 were detected with a high intensity after negative ionization, A_8 signal being the most intense among the metabolites when considering both ionization modes. Although A_5, A_6, and A_8 were not detected when re-extracting the urine samples after β-glucuronidase hydrolysis along with controls, the corresponding non-conjugated metabolites were not detected.

Case #2: 3- and 4-CMC-Positive Oral Fluid

3-CMC metabolites A_1, A_2, A_3, A_4, A_7, and A_8 were detected in the oral fluid of case #2, along with the parent; no additional metabolite was identified. 3-CMC, A_1 (β-ketoreduction and *N*-demethylation), and A_3 (β-ketoreduction) had the most intense signals. 4-CMC metabolites B_1, B_2, B_3, and B_4 were detected, along with the parent, and B_4 (β-ketoreduction) was preponderant.

Case #3: 4-CMC-Positive Urine

Except for B_7, all 4-CMC metabolites identified in human hepatocyte incubations were also detected in the urine of case #3, along with the parent. An additional minor metabolite (B_A) produced by hydroxylation (+O) and glucuronidation ($+C_6H_8O_6$) was identified in urine, as suggested by the +192.0272 Da mass shift from 4-CMC and its fragmentation that is similar to that of the corresponding non-conjugated metabolite B_7. B_A was retrospectively detected in human hepatocyte incubates, although with an intensity below the established threshold. 4-CMC and B_4 (β-ketoreduction) had the most intense signal in positive-ionization mode, and B_5 (*N*-demethylation and ω-carboxylation), B_6 (β-ketoreduction, oxidative deamination, and *O*-glucuronidation), B_8 (β-ketoreduction, oxidative deamination, and *O*-glucuronidation), and B_9 (β-ketoreduction, oxidative deamination, and *O*-glucuronidation) were major after negative ionization, B_5 signal being the most intense among the metabolites when considering both ionization modes. B_6, B_8, and B_9 corresponding non-conjugated forms were not detected after glucuronide hydrolysis in urine.

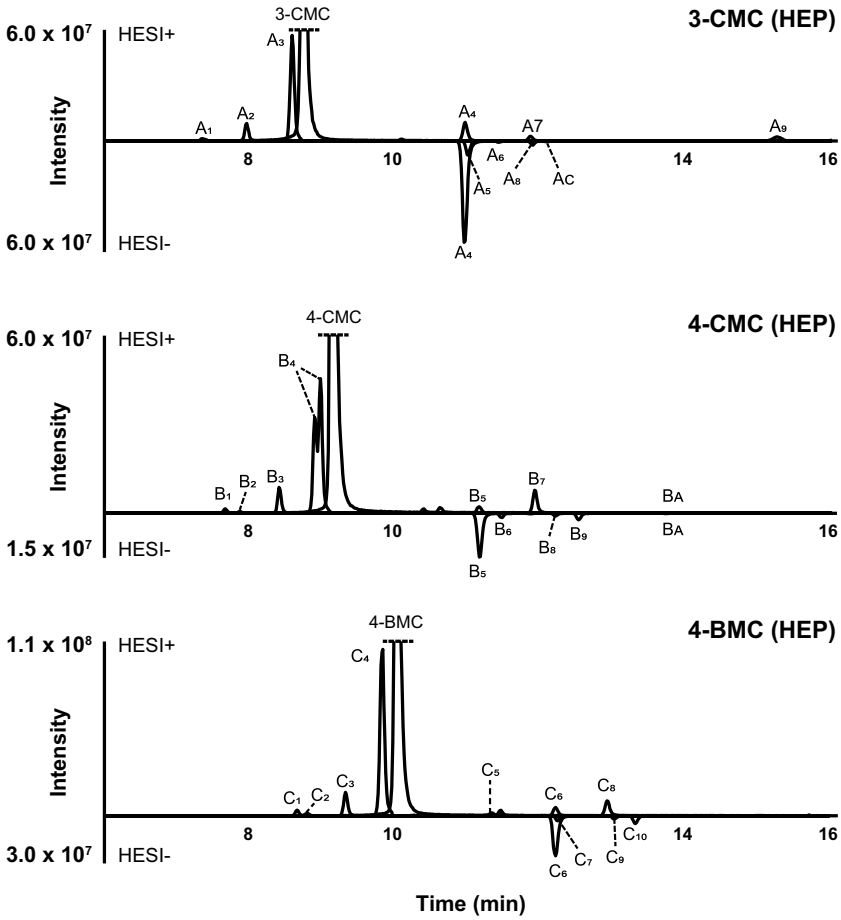

Fig. 5 Extracted-ion chromatograms of 3-CMC, 4-CMC, 4-BMC, and metabolites identified in human hepatocyte incubates. Mass tolerance, 5 ppm

Discussion

The abundance of the metabolites cannot be accurately determined under the present analytical conditions due to the lack of analytical standards for the metabolites identified. UV detection might have more accurately reflected the relative amount of the metabolites, although its sensitivity might have been a limiting parameter. The comparison can therefore only be based on the relative signal intensity of the analytes, which can be affected by sample preparation, matrix effect, and susceptibility to electrospray ionization. This latter bias is particularly critical in the present study as major metabolites detected in negative-ionization mode, and produced by combination of β-ketoreduction, oxidative deamination, and *O*-glucuronidation, are not ionized in positive mode and therefore not detected. Additionally, the ionization of these major metabolites in negative-ionization mode being due to the carboxylic acid group of the glucuronide, the corresponding non-conjugated metabolites (β-ketoreduction and oxidative deamination) and all metabolites that undergo oxidative deamination might have been produced, but were not detected under the present analytical conditions. This hypothesis is corroborated by the non-detection of the corresponding non-conjugated metabolites (and the conjugated ones) in hydrolyzed urine.

The three cathinones displayed a similar metabolic fate, as shown in Fig. 7.

In Vitro Versus in Vivo

Hepatocyte incubations are a good model to predict *in vivo* metabolism, although they do not reproduce all processes such as extrahepatic metabolism, reabsorption, and enterohepatic circulation. However, good correlation between 3-CMC incubation with human hepatocytes and authentic samples from cases #1 and #2 was found, as the same metabolites were identified except for A_A and A_B (β-ketoreduction and glucuronidation), which were only detected in the urine of case #1, albeit with a low intensity compared to the other metabolites, and A_9 (β-ketoreduction and *N*-acetylation), which was only detected *in vitro*. In postmortem case #1, 3-CMC was not detected in blood and its signal was low in urine compared to that of the main metabolites, which may indicate that a long time elapsed between consumption and death. Consistent with *in vitro* results, the metabolites with the most intense signal in urine and blood were produced

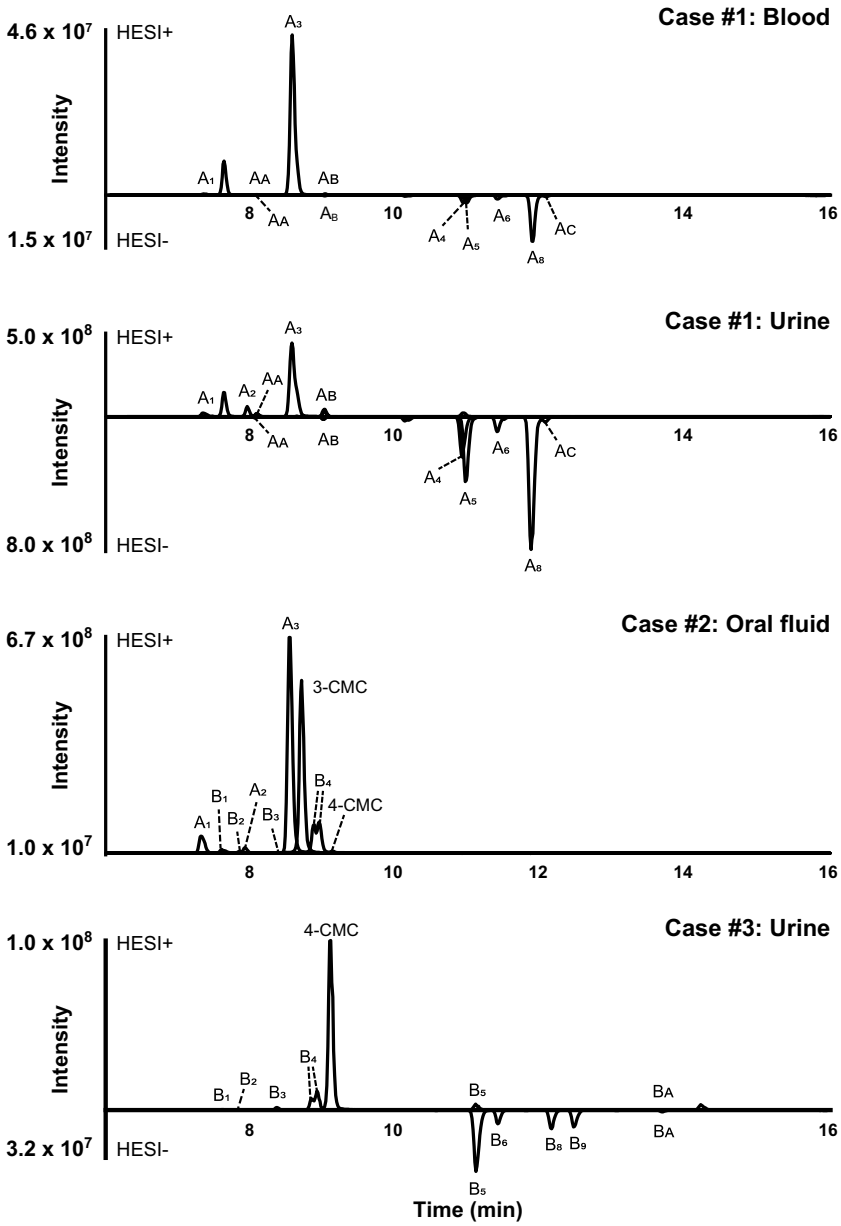

Fig. 6 Extracted-ion chromatograms of 3-CMC, 4-CMC, and metabolites identified in authentic samples. Mass tolerance, 5 ppm

through β-ketoreduction (A_3) in positive-ionization mode; β-ketoreduction, oxidative deamination, and further *O*-glucuronidation (A_5, A_6, and A_8), and *N*-demethylation and ω-carboxylation (A_4), when considering the signal in negative-ionization mode. In case #2 oral fluid, 3-CMC was intense, pointing towards a recent consumption, and A_3 (β-ketoreduction) was the only major metabolite.

Good correlation was also found between 4-CMC *in vitro versus in vivo* samples, despite B_7 (ω-hydroxylation) being major in incubates but not detected in authentic samples. Conversely, 4-CMC was intense in case #3 urine, and metabolites B_4 (β-ketoreduction) in positive-ionization mode and B_8 and B_9 (β-ketoreduction, oxidative deamination, and *O*-glucuronidation) after negative ionization, were predominant. Of note, in case #2, the distinction between 3- and 4-CMC metabolites with the same transformations was only possible through their retention times as determined *in vitro*, considering that they yield the same fragments with similar relative intensities.

Comparison to the Literature

In the present study, 3-CMC, 4-CMC, and 4-BMC human metabolism was investigated with *in silico* metabolite prediction, human hepatocyte incubations, and authentic positive samples for a comprehensive overview. The samples were analyzed by LC-HRMS/MS and targeted and untargeted data mining strategy for an exhaustive screening.

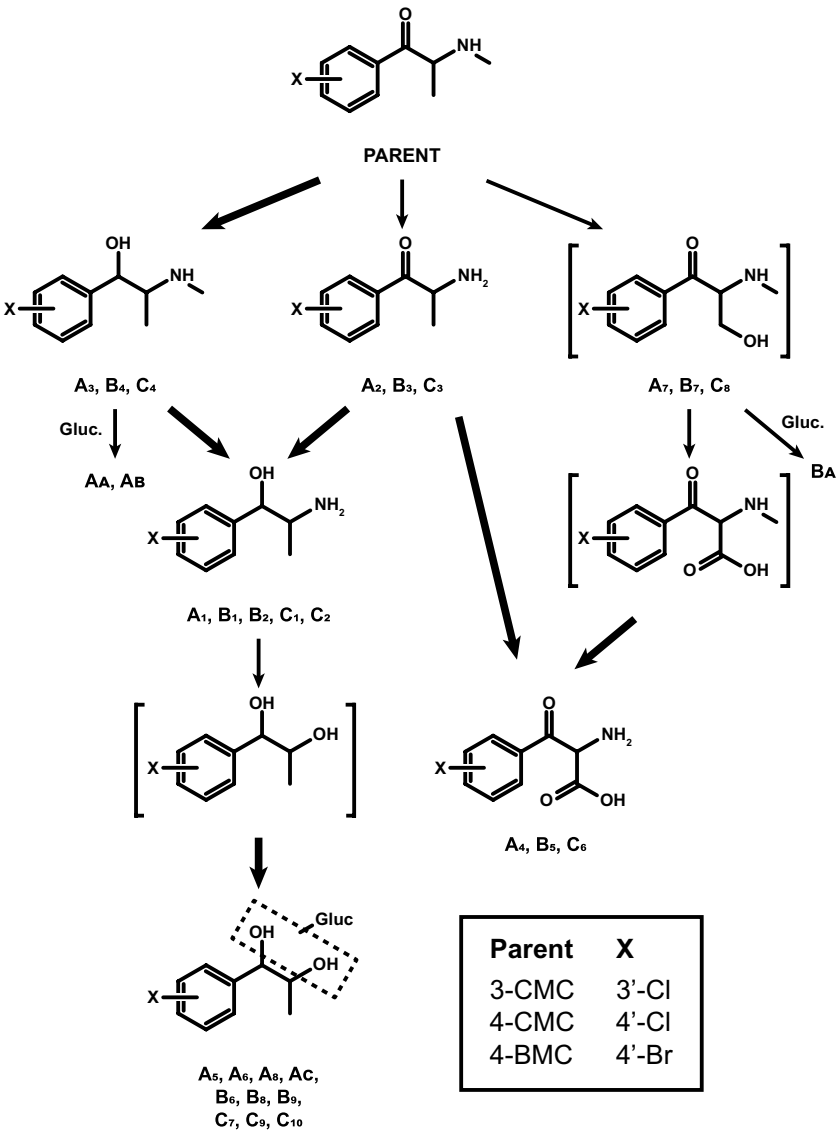

Fig. 7 3-CMC, 4-CMC, and 4-BMC metabolic fate in humans. Gluc, glucuronide; bold arrows indicate major pathways

3-CMC metabolism was previously studied using human liver microsomes by Lopes *et al.* (5) and in a case report by Romańczuk *et al.* (16). 4-CMC metabolism also was recently assessed by Massano *et al.* during a clinical study with several participants (18). Consistent with our results, the authors found that β-ketoreduction and *N*-demethylation were major 3- and 4-CMC metabolic pathways. However, none of the studies reported the detection of metabolites formed through *N*-demethylation and ω-carboxylation (A_4 and B_5), or β-ketoreduction, oxidative deamination, and *O*-glucuronidation (A_5, A_6, A_8, A_C, B_6, B_8, and B_9), although A_4, A_8, B_6, B_8, and B_9 were major in our study, especially in urine where A_8 and B_5 were the main metabolites in cases #1 and #3, respectively. In the study by Lopes *et al.*, 3-CMC metabolism was assessed using human liver microsome incubations without authentic samples, which are a good first approach in identifying the metabolites of specific molecules but do not contain all hepatic enzymes and endogenous cofactors and do not provide the natural orientation of membrane enzymes (5). In the studies by Romańczuk *et al.* and Massano *et al.*, the analyses were conducted by LC-MS/MS in after electrospray ionization in positive mode only (16,18), which may explain why A_4 and B_5 (higher signal in negative-ionization mode) and A_5, A_6, A_8, A_C, B_6, B_8, and B_9 (no signal in positive-ionization mode) were not detected. In the three articles, the approach used for data mining was not described and the metabolites might have been not detected because they were simply not expected and therefore not searched. Noteworthy, the corresponding metabolites were never reported in the metabolism of other popular SCs such as 3- and 4-MMC, although the same transformation can theoretically occur (27–29). This highlights the need for a comprehensive screening of the data with targeted and untargeted strategies for metabolic

identification studies, in general. Further comparison is complicated by the lack of detailed information regarding metabolite intensities.

Markers of Consumption

β-Ketoreduction was a major metabolic transformation in all the biological matrices analyzed, consistent with the metabolism of cathinones in general (30). Phase I metabolites with a combination of *N*-demethylation and ω-carboxylation and phase II metabolites with a combination of β-ketoreduction, oxidative deamination, and *O*-glucuronidation also had an intense signal, especially in negative-ionization mode. Based on our *in vitro* and *in vivo* findings, we suggest A_3, A_4, and A_8 in blood; A_3, A_4, A_5, and A_8 in urine; and A_3 in oral fluid; as specific metabolite marker of 3-CMC consumption. Similarly, we suggest B_4 and B_5 in blood; B_4, B_5, B_6, B_8, and B_9 in urine; and B_4 in oral fluid; as metabolite markers of 4-CMC use. Due to the similar metabolic profile *in vitro*, we suggest the corresponding metabolites C_4 and C_6 in blood; C_4, C_6, C_7, C_9, and C_{10} in urine; and C_4 in oral fluid; as markers of 4-BMC use. The parent signal should also be monitored in cases or recent consumption. Careful attention should be taken to separate position isomers 3-CMC, 4-CMC, and their metabolites to avoid misidentification. Glucuronide hydrolysis of urine samples is not recommended, as the corresponding non-conjugated compounds were not detected with present analytical conditions.

Conclusions

We identified alternative major metabolites markers for documenting 3- and 4-CMC intake in clinical and forensic casework, and we investigated 4-BMC metabolism for the first time. Several major metabolites were poorly or even not detected after positive electrospray ionization, which is often the only ionization mode used in metabolite identification studies. Additionally, several major urinary metabolites were glucuronides whose non-conjugated forms are unlikely to be detected after electrospray ionization, although the analysis of urine samples only after glucuronide hydrolysis is often performed in this kind of studies. We therefore recommend toxicologists being cautious when interpreting data from hydrolyzed samples during routine drug screening, as major metabolites might have become undetectable.

Moreover, our results strongly support the need for comprehensive screening strategies in metabolite identification studies, to avoid overlooking important metabolites. Orthogonal data obtained from different types of analysis, i.e., different analytical columns, ionization modes, or even technologies, are especially paramount. Further investigation in the metabolism of other popular methcathinone analogues such as 3- and 4-MMC is needed, as the corresponding metabolites might be produced.

Supplementary Information The online version contains supplementary material available at https://doi.org/10.1208/s12248-024-00940-8.

Author Contribution Conceptualization, D.B., F.P.B., and J.C.; methodology, D.B. and J.C.; formal analysis, D.B. and J.C.; investigation, D.B. and J.C.; resources, G.R., L.P.T., P.A., and F.P.B.; data curation, D.B., O.T., G.D., F.T., and J.C.; writing—original draft preparation, D.B., O.T., G.D., F.T., and J.C.; writing—review and editing, G.R., L.P.T., P.A., and F.P.B.; visualization, D.B., O.T., G.D., F.T., and J.C.; supervision, J.C.; project administration, F.P.B. and J.C.; funding acquisition, F.P.B. All authors have read and agreed to the published version of the manuscript.

Funding Open access funding provided by Università Politecnica delle Marche within the CRUI-CARE Agreement. This research was funded by the Department for Drug Policies, in Italy, under the project's names "Effetti delle NPS: Sviluppo di una multicentrica di ricerca per il potenziamento informativo del Sistema di Allerta Precoce" and "SNAP".

Data Availability Derived data supporting the findings of this study are available from the corresponding author on request.

Declarations

Conflict of Interest The authors declare no competing interests.

References

1. Daziani G, Lo Faro AF, Montana V, Goteri G, Pesaresi M, Bambagiotti G, *et al*. Synthetic cathinones and neurotoxicity risks: a systematic review. Int J Mol Sci. 2023;24:6230. https://doi.org/10.3390/ijms24076230.
2. European Monitoring Centre for Drugs and Drug Addiction. European Drug Report 2023: Trends and Developments 2024. https://www.emcdda.europa.eu/publications/european-drug-report/2023_en. Accessed 25 Mar 2024.
3. Carlier J, Berardinelli D, Montanari E, Sirignano A, Di Trana A, Busardò FP. 3F-α-pyrrolydinovalerophenone (3F-α-PVP) *in vitro* human metabolism: multiple *in silico* predictions to assist in LC-HRMS/MS analysis and targeted/untargeted data mining. J Chromatogr B. 2022;1193:123162. https://doi.org/10.1016/j.jchromb.2022.123162.
4. Nadal-Gratacós N, Lleixà E, Gibert-Serramià M, Estrada-Tejedor R, Berzosa X, Batllori X, *et al*. Neuropsychopharmacology of emerging drugs of abuse: Meta- and Para-halogen-ring-substituted

α-PVP ("flakka") derivatives. Int J Mol Sci. 2022;23:2226. https://doi.org/10.3390/ijms23042226.
5. Lopes RP, Ferro RA, Milhazes M, Figueira M, Caldeira MJ, Antunes AMM, *et al*. Metabolic stability and metabolite profiling of emerging synthetic cathinones. Front Pharmacol. 2023;14:1–14. https://doi.org/10.3389/fphar.2023.1145140.
6. La Maida N, Di Trana A, Giorgetti R, Tagliabracci A, Busardò FP, Huestis MA. A review of synthetic cathinone–related fatalities from 2017 to 2020. Ther Drug Monit. 2021;43:52–68. https://doi.org/10.1097/FTD.0000000000000808.
7. Suyama JA, Sakloth F, Kolanos R, Glennon RA, Lazenka MF, Negus SS, *et al*. Abuse-related neurochemical effects of Para-substituted methcathinone analogs in rats: microdialysis studies of nucleus accumbens dopamine and serotonin. J Pharmacol Exp Ther. 2016;356:182–90. https://doi.org/10.1124/jpet.115.229559.
8. Luethi D, Walter M, Zhou X, Rudin D, Krähenbühl S, Liechti ME. Para-halogenation affects monoamine transporter inhibition properties and hepatocellular toxicity of amphetamines and methcathinones. Front Pharmacol. 2019;10:1–9. https://doi.org/10.3389/fphar.2019.00438.
9. Klavž J, Gorenjak M, Marinšek M. Suicide attempt with a mix of synthetic cannabinoids and synthetic cathinones: case report of non-fatal intoxication with AB-CHMINACA, AB-FUBINACA, alpha-PHP, alpha-PVP and 4-CMC. Forensic Sci Int. 2016;265:121–4. https://doi.org/10.1016/j.forsciint.2016.01.018.
10. Grifell M, Ventura M, Carbón X, Quintana P, Galindo L, Palma Á, *et al*. Patterns of use and toxicity of new Para-halogenated substituted cathinones: 4-CMC (clephedrone), 4-CEC (4-chloroethcatinone) and 4-BMC (brephedrone). Hum Psychopharmacol. 2017;32:1–9. https://doi.org/10.1002/hup.2621.
11. Wiergowski M, Aszyk J, Kaliszan M, Wilczewska K, Anand JS, Kot-Wasik A, *et al*. Identification of novel psychoactive substances 25B-NBOMe and 4-CMC in biological material using HPLC-Q-TOF-MS and their quantification in blood using UPLC–MS/MS in case of severe intoxications. J Chromatogr B. 2017;1041–1042:1–10. https://doi.org/10.1016/j.jchromb.2016.12.018.
12. Tomczak E, Woźniak MK, Kata M, Wiergowski M, Szpiech B, Biziuk M. Blood concentrations of a new psychoactive substance 4-chloromethcathinone (4-CMC) determined in 15 forensic cases. Forensic Toxicol. 2018;36:476–85. https://doi.org/10.1007/s11419-018-0427-8.
13. Adamowicz P, Jurczyk A, Gil D, Szustowski S. A case of intoxication with a new cathinone derivative α-PiHP – a presentation of concentrations in biological specimens. Legal Med. 2020;42:101626. https://doi.org/10.1016/j.legalmed.2019.101626.
14. Woźniak MK, Banaszkiewicz L, Aszyk J, Wiergowski M, Jańczewska I, Wierzba J, *et al*. Development and validation of a method for the simultaneous analysis of fatty acid ethyl esters, ethyl sulfate and ethyl glucuronide in neonatal meconium: application in two cases of alcohol consumption during pregnancy. Anal Bioanal Chem. 2021;413:3093–105. https://doi.org/10.1007/s00216-021-03248-0.
15. Tusiewicz K, Chłopaś-Konowałek A, Wachełko O, Zawadzki M, Szpot P. A fatal case involving the highest ever reported 4-CMC concentration. J Forensic Sci. 2023;68:349–54. https://doi.org/10.1111/1556-4029.15162.
16. Romańczuk A, Rojek S, Synowiec K, Maciów-Głąb M, Kula K, Rzepecka-Woźniak E. The stability of synthetic cathinones and the study of potential intake biomarkers in the biological material from a case of 3-CMC poisoning. J Anal Toxicol. 2023;47:470–80. https://doi.org/10.1093/jat/bkad010.
17. Uralets V, Rana S, Morgan S, Ross W. Testing for designer stimulants: metabolic profiles of 16 synthetic cathinones excreted free in human urine. J Anal Toxicol. 2014;38:233–41. https://doi.org/10.1093/jat/bku021.
18. Massano M, Nuñez-Montero M, Papaseit E, Hladun O, Pérez-Maña C, Ventura M, *et al*. Metabolic profile of N-ethylhexedrone, N-ethylpentedrone, and 4-chloromethcathinone in urine samples by UHPLC-QTOF-HRMS. J Pharm Biomed Anal. 2024;241:115994. https://doi.org/10.1016/j.jpba.2024.115994.
19. Stork C, Embruch G, Šícho M, de Bruyn KC, Chen Y, Svozil D, *et al.* NERDD: a web portal providing access to *in silico* tools for drug discovery. Bioinformatics. 2020;36:1291–2. https://doi.org/10.1093/bioinformatics/btz695.
20. De Bruyn KC, Šícho M, Mazzolari A, Kirchmair J. GLORYx: prediction of the metabolites resulting from phase 1 and phase 2 biotransformations of xenobiotics. Chem Res Toxicol. 2021;34:286–99. https://doi.org/10.1021/acs.chemrestox.0c00224.
21. Di Trana A, Brunetti P, Giorgetti R, Marinelli E, Zaami S, Busardò FP, *et al*. *In silico* prediction, LC-HRMS/MS analysis, and targeted/untargeted data-mining workflow for the profiling of phenylfentanyl *in vitro* metabolites. Talanta. 2021;235:122740. https://doi.org/10.1016/J.TALANTA.2021.122740.
22. Keller BO, Sui J, Young AB, Whittal RM. Interferences and contaminants encountered in modern mass spectrometry. Anal Chim Acta. 2008;627:71–81. https://doi.org/10.1016/j.aca.2008.04.043.
23. Brunetti P, Lo Faro AF, Di Trana A, Montana A, Basile G, Carlier J, *et al*. β′-Phenylfentanyl metabolism in primary human hepatocyte incubations: identification of potential biomarkers of exposure in clinical and forensic toxicology. J Anal Toxicol. 2023;46:e207–17. https://doi.org/10.1093/JAT/BKAC065.
24. Carlier J, Diao X, Giorgetti R, Busardò FP, Huestis MA. Pyrrolidinyl synthetic Cathinones α-PHP and 4F-α-PVP metabolite profiling using human hepatocyte incubations. Int J Mol Sci. 2021;22:1–17. https://doi.org/10.3390/ijms22010230.
25. Busardò FP, Lo Faro AF, Sirignano A, Giorgetti R, Carlier J. *In silico*, *in vitro*, and *in vivo* human metabolism of acetazolamide, a carbonic anhydrase inhibitor and common "diuretic and masking agent" in doping. Arch Toxicol. 2022;96:1989–2001. https://doi.org/10.1007/s00204-022-03289-z.
26. Carlier J, Malaca S, Huestis MA, Tagliabracci A, Tini A, Busardò FP. Biomarkers of 4-hydroxy-N,N- methylpropyltryptamine (4-OH-MPT) intake identified from human hepatocyte incubations. Expert Opin Drug Metab Toxicol. 2022;18:831–40. https://doi.org/10.1080/17425255.2022.2166826.
27. Khreit OIG, Grant MH, Zhang T, Henderson C, Watson DG, Sutcliffe OB. Elucidation of the phase I and phase II metabolic pathways of (±)-4′-methylmethcathinone (4-MMC) and (±)-4′-(trifluoromethyl)methcathinone (4-TFMMC) in rat liver hepatocytes using LC–MS and LC–MS2. J Pharm Biomed Anal. 2013;72:177–85. https://doi.org/10.1016/j.jpba.2012.08.015.
28. Aknouche F, Ameline A, Gheddar L, Maruejouls C, Kintz P. Fatal rectal injection of 3-MMC in a sexual context: toxicological investigations including metabolites identification using LC–HRMS. J Anal Toxicol. 2022;46:949–55. https://doi.org/10.1093/jat/bkac048.
29. Che P, Davidson JT, Still K, Kool J, Kohler I. *In vitro* metabolism of cathinone positional isomers: does sex matter? Anal Bioanal Chem. 2023;415:5403–20. https://doi.org/10.1007/s00216-023-04815-3.
30. Tyrkkö E, Andersson M, Kronstrand R. The toxicology of new psychoactive substances. Ther Drug Monit. 2016;38:190–216. https://doi.org/10.1097/FTD.0000000000000263.